shows that Hcy inhibits apoE3 dimerization, which impairs HDL generation, there is no difference in the level of HDL-cholesterol between the samples from patients with hyperhomocysteinemia and normal Hcy. This is because apolipoprotein AI, but not apoE, plays a major role in HDL generation in systemic circulation. There is a negative correlation between the ratio of apoE3 dimer and the level of plasma total cholesterol; however, it is unlikely that there is a cause-and-effect relationship between these two parameters. Because cholesterol metabolism in the brain is separated from that of systemic circulation by the blood-brain barrier, the cholesterol level in the plasma does not correlate with that in the brain. Thus, it is necessary to determine the lipid profile, including apoE-mediated HDL generation, in CSF in a future study.

Supplementl Figure 1
Minagawa et al

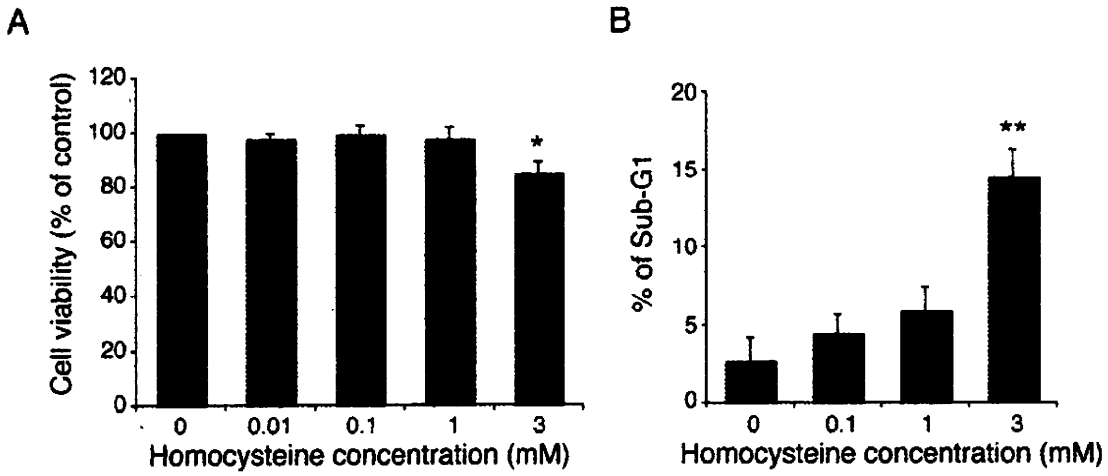

Supplemental Figure 2

Minagawa et al

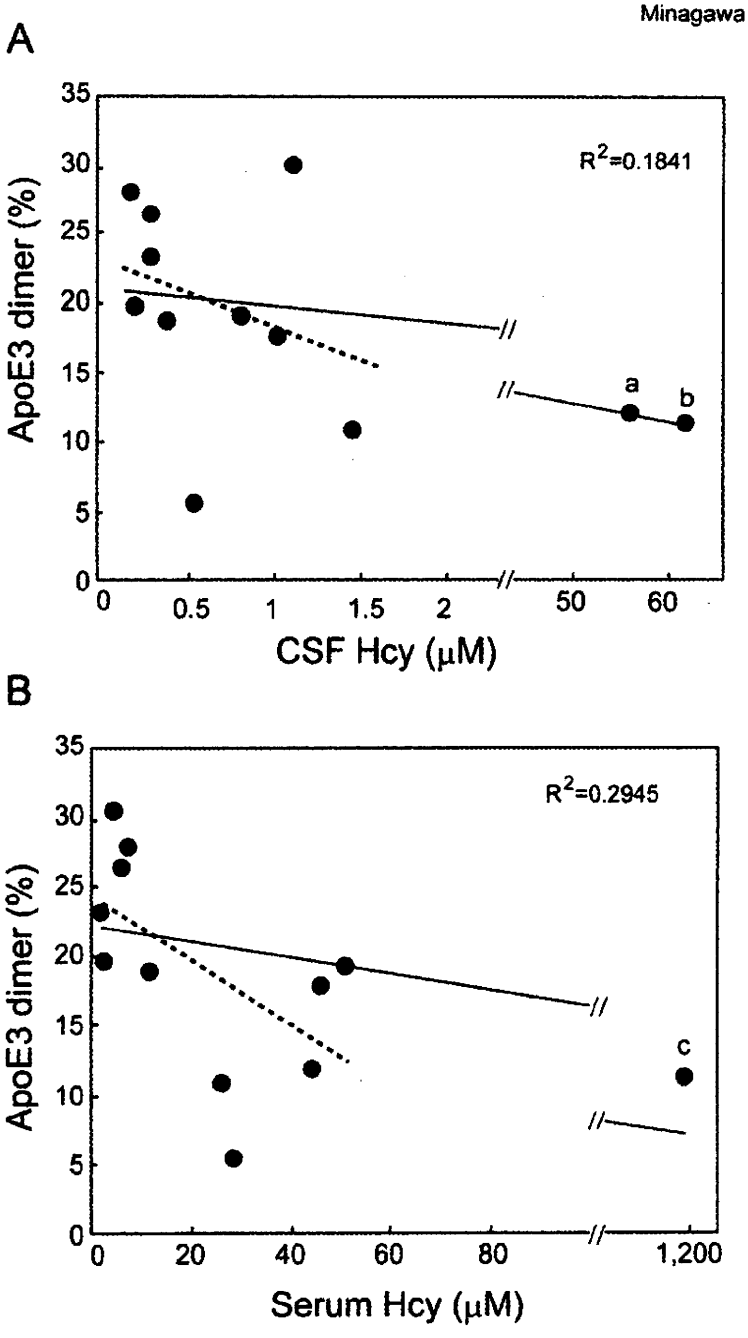

Supplemental Figure 3

Minagawa et al

A

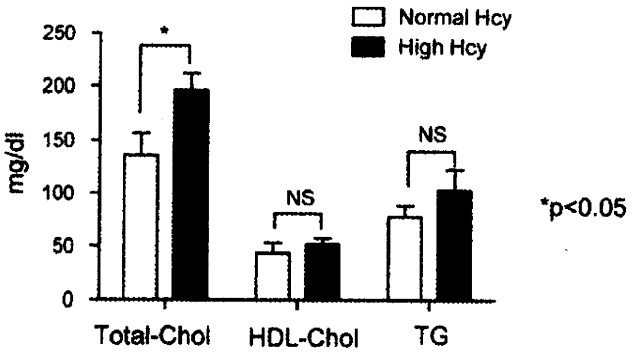

*p<0.05

B

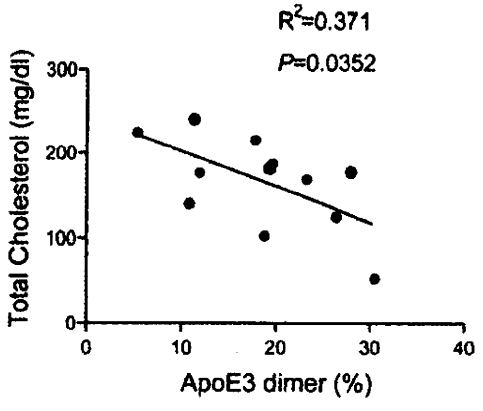

C

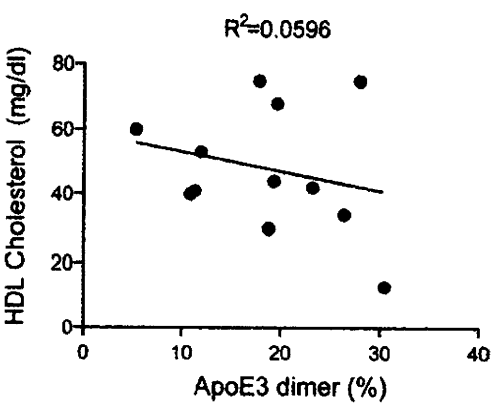

D

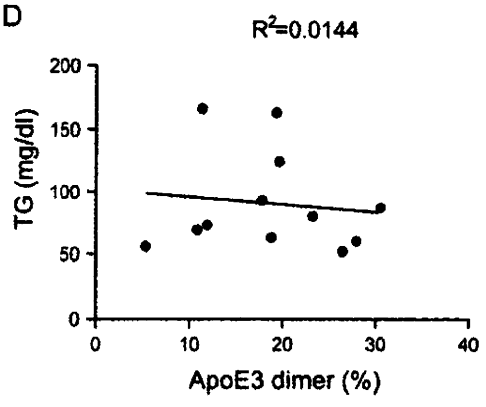

Supplemental Table 1. Plasma lipid profile of the patients

	NO	Total cholesterol (mg/dl)	HDL-cholesterol (mg/dl)	Triglyceride (mg/dl)
Normal Hcy	1	55	13	87
	2	103	30	63
	3	168	42	80
	4	124	34	52
	5	177	75	60
	6	187	68	125
High Hcy	7	176	53	73
	8	181	44	163
	9	241	41	166
	10	216	75	93
	11	139	40	69
	12	225	60	56

THE JOURNAL OF BIOLOGICAL CHEMISTRY VOL. 286, NO. 8, pp. 6393–6401, February 25, 2011

Lipoprotein Lipase Is a Novel Amyloid β (Aβ)-binding Protein That Promotes Glycosaminoglycan-dependent Cellular Uptake of Aβ in Astrocytes*[S]

Received for publication, August 4, 2010, and in revised form, November 23, 2010 Published, JBC Papers in Press, December 21, 2010, DOI 10.1074/jbc.M110.172106

Kazuchika Nishitsuji[‡], Takashi Hosono[‡], Kenji Uchimura[‡§], and Makoto Michikawa[‡1]

From the [§]Section of Pathophysiology and Neurobiology, [‡]Department of Alzheimer's Disease Research, National Center for Geriatrics and Gerontology, Obu, Aichi 474-8511, Japan

Lipoprotein lipase (LPL) is a member of a lipase family known to hydrolyze triglyceride molecules in plasma lipoprotein particles. LPL also plays a role in the binding of lipoprotein particles to cell-surface molecules, including sulfated glycosaminoglycans (GAGs). LPL is predominantly expressed in adipose and muscle but is also highly expressed in the brain where its specific roles are unknown. It has been shown that LPL is colocalized with senile plaques in Alzheimer disease (AD) brains, and its mutations are associated with the severity of AD pathophysiological features. In this study, we identified a novel function of LPL; that is, LPL binds to amyloid β protein (Aβ) and promotes cell-surface association and uptake of Aβ in mouse primary astrocytes. The internalized Aβ was degraded within 12 h, mainly in a lysosomal pathway. We also found that sulfated GAGs were involved in the LPL-mediated cellular uptake of Aβ. Apolipoprotein E was dispensable in the LPL-mediated uptake of Aβ. Our findings indicate that LPL is a novel Aβ-binding protein promoting cellular uptake and subsequent degradation of Aβ.

Lipoprotein lipase (LPL)[2] catalyzes the hydrolysis of triacylglycerol and mediates the cellular uptake of lipoproteins by functioning as a "bridging molecule" between lipoproteins and sulfated glycosaminoglycans (GAGs) or lipoprotein receptors in blood vessels (1, 2). Sulfated GAGs are side chains of proteoglycans normally found in the extracellular matrix and on the cell surface in the peripheral tissues and brain. Sulfation modifications vary within the GAG chains and are crucial for interaction between GAGs and various protein ligands (3), including LPL (4, 5).

It has been shown that LPL is distributed in numerous organs and is highly expressed in the brain (6, 7). Although the catabolic activity of LPL on triacylglycerol is observed in the brain (8), the finding that apolipoprotein CII (apoCII), an essential cofactor for LPL, is not expressed in the brain (9, 10), suggests that LPL has a novel nonenzymatic function in the brain. However, little is known about LPL function in the brain. Interestingly, it has been shown that LPL is accumulated in senile plaques of Alzheimer disease (AD) brains (11). Moreover, SNPs in the coding region of the LPL gene are associated with disease incidence in clinically diagnosed AD subjects, LPL mRNA expression level, brain cholesterol level, and the severity of AD pathologies, including neurofibrillary tangles and senile plaque density (12). These results suggest that LPL may have a physiological role in the brain, whose alternation is associated with the pathogenesis of AD.

The occurrence of senile plaques in the brain is one of the pathological hallmarks of AD. They contain extracellular deposits of amyloid β protein (Aβ), and the abnormal Aβ deposition or the formation of soluble Aβ oligomers is crucial for AD pathogenesis. Aβ is a physiological peptide whose main species are 40 and 42 amino acids in length, and Aβ42 is the predominant specie in senile plaques (13). The Aβ levels are determined by the balance between its production and degradation/clearance, and an attenuated Aβ catabolism is suggested to cause Aβ accumulation in aging brains (14). Previous studies have shown that astrocytes and microglia directly take up and degrade Aβ42 (15, 16) and that Aβ degradation occurs in late endosomal-lysosomal compartments (17, 18). These lines of evidence, together with the finding that LPL mediates the cellular uptake of lipoproteins (1, 2), led us to carry out experiments to determine whether LPL interacts with Aβ to promote Aβ cellular uptake and degradation in astrocytes. Here, we provide evidence that LPL forms a complex with Aβ and facilitates Aβ cell surface binding and uptake in mouse primary astrocytes through a mechanism that is dependent on heparan sulfate and chondroitin sulfate GAG chains, leading to the lysosomal degradation of Aβ.

MATERIALS AND METHODS

Materials—Bovine LPL, heparinases, and a polyclonal anti-actin antibody were purchased from Sigma. Synthetic Aβ1–42 was purchased from the Peptide Institute (Osaka,

* This work was supported by a grant-in-aid for scientific research on priority areas (Research on Pathomechanisms of Brain Disorders) from the Ministry of Education, Culture, Sports, Science, and Technology of Japan, a grant from the Program for Promotion of Fundamental Studies in Health Sciences of the National Institute of Biomedical Innovation, a grant from the Ministry of Health, Labor, and Welfare of Japan (Research on Dementia, Health, and Labor Sciences Research Grant H20-007), and a grant from the Japan Health Sciences Foundation (Research on Publicly Essential Drugs and Medical Devices).

[S] The on-line version of this article (available at http://www.jbc.org) contains supplemental "Methods" and Fig. 1.

[1] To whom correspondence should be addressed: Department of Alzheimer's Disease Research, National Center for Geriatrics and Gerontology, Gengo 35, Morioka, Obu, Aichi 474-8511, Japan. Tel.: 81-562-46-2311; Fax: 81-562-46-8569; E-mail: michi@ncgg.go.jp.

[2] The abbreviations used are: LPL, lipoprotein lipase; Aβ, amyloid β; ApoE, apolipoprotein E; CS, chondroitin sulfate(s); HS, heparan sulfate; GAG, glycosaminoglycan; ANOVA, one-way analysis of variance.

Japan). Heparin, chondroitin, chondroitin sulfates, and chondroitinase ABC were from Seikagaku (Tokyo, Japan). Monoclonal anti-Aβ antibodies (6E10, 4G8) were purchased from Signet Laboratories (Dedham, MA), and a goat polyclonal anti-ApoE antibody and mouse control IgG were from Millipore (Bedford, MA). An anti-LPL antibody and Cy3- and FITC- conjugated secondary antibodies were purchased from Abcam, Inc. (Cambridge, MA). A monoclonal anti-Aβ antibody (2C8) was purchased from Medical and Biological Laboratories (Nagoya, Japan).

Animals—C57BL/6 mice were purchased from SLC, Inc. (Hamamatsu, Japan). ApoE-KO mice were obtained from Jackson ImmunoResearch Laboratories (Bar Harbor, ME). The National Center of Geriatrics and Gerontology Institutional Animal Care and Use Committee approved the animal studies.

Preparation of LPL—Because the sequence of LPL is highly conserved among mammalian species and the ability of LPL to interact with proteoglycans is also well conserved, we used LPL purified from bovine milk. An LPL suspension (suspended in 3.8 M ammonium sulfate, 0.02 M Tris-HCl, pH 8.0) was centrifuged (10,000 × *g* for 20 min at 4 °C), and the resulting pellet was dissolved in PBS. The prepared LPL was stored at 4 °C and used within 3 days.

Cell Culture—Highly astrocyte-rich cultures were prepared according to a method described previously (19). In brief, brains of postnatal day 2 C57BL/6 mice or ApoE knock-out mice were removed under anesthesia. The cerebral cortices from the mouse brains were dissected, freed from meninges, and diced into small pieces; the cortical fragments were incubated in 0.25% trypsin and 20 mg/ml DNase I in PBS at 37 °C for 20 min. The fragments were then dissociated into single cells by pipetting. The dissociated cells were seeded in 75-cm^2 dishes at a density of 5×10^7 cells per flask in DMEM-containing 10% FBS. After 10 days of incubation *in vitro*, flasks were shaken at 37 °C overnight, and the remaining astrocytes in the monolayer were trypsinized (0.1%) and reseeded. The astrocyte-rich cultures were maintained in DMEM-containing 10% FBS until use.

Assay of Aβ Binding and Uptake in Astrocytes by Western Blotting—Assays were carried out on confluent monolayers of astrocytes grown in 12-well plates. Aβ was dissolved in dimethyl sulfoxide to a final concentration of 1 mM and stored at −40 °C. Aβ (500 nM) and LPL (1–10 μg/ml) were mixed in DMEM. Immediately, the mixture was added to the culture medium of astrocytes. Cells were incubated at 37 °C for 5 h to assess the cellular uptake of Aβ or at 4 °C for 3 h to evaluate the binding of Aβ to the cell surface of astrocytes. In these assays, cells were incubated in serum-free DMEM. After incubation, cells were washed with PBS three times, harvested using a cell scraper and lysed by sonication in radioimmune precipitation assay buffer (1% Nonidet P-40, 0.5% sodium deoxycholate, 0.1% SDS, 150 mM NaCl, 50 mM Tris-HCl (pH 8.0), 1 mM EDTA). Cell lysates were subjected to SDS-PAGE with 4–20% gradient gels (WAKO Pure Chemicals, Osaka, Japan) and transferred to polyvinylidene difluoride membranes (Millipore). Aβ was probed with 6E10 antibody followed by horseradish peroxidase-labeled anti-mouse antibody (Cell Signaling Technology, Inc., Beverly, MA) and chemiluminescent substrate ECL Plus (GE Healthcare). The protein contents of cell lysates were normalized to the expression level of actin protein. To examine the involvement of GAGs, heparin, chemically modified heparins, chondroitin, or chondroitin sulfates (3 μg/ml) were incubated with a mixture solution of Aβ and LPL. Astrocytes were pretreated with a mixture of heparinase II and heparinase III or chondroitinase ABC (0.03 units/ml) for 24 h at 37 °C to evaluate endogenously expressed glycosaminoglycans. Signals were visualized and quantified using a LAS-3000 luminescent image analyzer (Fujifilm, Tokyo, Japan) and ImageJ software (National Institutes of Health, Bethesda, MD). For analyzing protein band densities, a region of interest was drawn around a band, and protein band densities were calculated.

siRNA Interference of LPL—siRNA specific for mouse LPL (sense strand, 5′-CAGCUGAGGACACUUGUCAUCUCAUdTdT-3′; antisense strand, 5′-AUGAGAUGACAAGUGUCCUCAGCUGdTdT-3′) and control siRNA (sense strand, 5′-CAGAGGGCACAUUUGACCUUUCCAUdTdT-3′; antisense strand, 5′-AUGGAAAGGUCAAAUGUGCCCUCUG-3′) was purchased from Invitrogen. Astrocytes grown in 12-well plates for 24 h were transfected with either LPL siRNA or control siRNA with Lipofectamine RNAiMAX (Invitrogen). Forty-eight hours after transfection, cells were treated with Aβ (1 μM) and then incubated at 4 °C for 3 h, and cell-surface associated Aβ was analyzed as described above. An anti-LPL antibody (Gene Tex, Inc.) was used for the detection of LPL.

Assay of Aβ Degradation in Astrocytes—Astrocytes were incubated with Aβ (250 nM) and LPL (2 μg/ml) at 37 °C for 5 h. Subsequently, cells were washed with DMEM and incubated in DMEM for additional hours. Then, Aβ in cell lysates was analyzed by Western blotting as described above.

Immunoprecipitation—Aβ (500 nM) and LPL at various concentrations were incubated in DMEM at 37 °C for 3 h. LPL-Aβ complexes were immunoprecipitated with an anti-LPL antibody and magnetic protein G beads (Dynal, Hamburg, Germany). For detection of LPL-Aβ complexes in the mice brains, brain homogenates from 12-week-old C57BL/6 mice were used. In brief, anesthetized mice were perfused with PBS containing 35 μg/ml heparin for 15 min. The cerebrum was dissected out and homogenized by sonication in 4 volumes of PBS containing a protease inhibitor mixture (P8340; Sigma) and centrifuged at 1,000 × *g* for 10 min at 4 °C. The supernatants were harvested and LPL-Aβ complexes were immunoprecipitated with an anti-LPL antibody and magnetic protein G beads. The obtained precipitates were washed three times with PBS and incubated at 70 °C for 10 min in SDS sample buffer. Dissociated Aβ recovered in the supernatant was assessed by Western blotting as described above. For detection of endogenous Aβ, the supernatants were subjected to SDS-PAGE with 4–20% gradient gels and transferred to polyvinylidene difluoride membranes. The membranes were exposed to microwave irradiation for 20 s, and Aβ was probed with 4G8 antibody followed by horseradish peroxidase-labeled anti-mouse antibody and the chemiluminescent substrate ECL Plus.

Immunocytochemistry—Astrocytes grown on poly-L-lysine-coated coverslips were incubated with a mixture of Aβ (250 nM) and LPL (2 μg/ml) at 37 °C for 5 h. After treatment, the cells were fixed with 4% paraformaldehyde in PBS at room temperature for 10 min, blocked, and permeabilized with 10% normal goat serum and 0.05% saponin in PBS at room temperature for 20 min. In some experiments, cells were washed twice with DMEM followed by incubation at 37 °C for 3 h in DMEM and fixed. The cells were then incubated with primary antibodies followed by Cy3- and FITC-conjugated secondary antibodies. The stained specimens were mounted with Fluor-Save reagents (Calbiochem) and examined under an LSM 510 confocal laser microscope (Carl Zeiss MicroImaging GmbH, Jena, Germany).

Statistical Analysis—The collected data were analyzed by one-way analysis of variance (ANOVA) including appropriate variables followed by the Dunnett's test or unpaired Student's *t* test. Results were considered significant when $p < 0.05$.

RESULTS

LPL Binds to Aβ in Vitro—LPL was incubated with freshly prepared Aβ42 *in vitro*, and the complexes formed were immunoprecipitated with an anti-LPL antibody coupled with magnetic beads, followed by probing Western blots of protein complexes using an anti-Aβ antibody (Fig. 1*A*). Aβ42 was immunoprecipitated with an anti-LPL antibody, but not with control IgG. The levels of Aβ42 recovered in the immunoprecipitates from samples in the presence of 2–5 μg/ml LPL were significantly higher than those from samples in the presence of 0, 0.5, or 1 μg/ml of LPL (Fig. 1, *B* and *C*), suggesting that LPL directly interacts with Aβ42, and these two molecules form a complex in an LPL dose-dependent manner. Furthermore, endogenous mouse Aβ was immunoprecipitated with the anti-LPL antibody from brain homogenates prepared from C57BL/6 mice (Fig. 1*D*), indicating that endogenous mouse LPL directly interacts with endogenous mouse Aβ. We also determined the assembly state of Aβ that forms complex with LPL. Solutions containing Aβ oligomers were subjected to immunoprecipitation/immunoblot analysis, and Aβ42 monomers were immunoprecipitated by an anti-LPL antibody (supplemental Fig. 1).

LPL Promotes Cell Surface Binding and Cellular Uptake of Aβ in Astrocytes—We then determined whether LPL affects the cellular binding of Aβ to astrocytes. Soluble Aβ42 and various concentrations of LPL were added to primarily cultured astrocytes prepared from WT mice and then incubated at 4 °C. LPL (2–5 μg/ml) of significantly augmented Aβ42 binding to astrocytes by 5.8- to 9-fold of that in the case without LPL (Fig. 2, *A* and *B*). To examine the effect of LPL on the cellular uptake of Aβ, we incubated primary astrocytes with soluble Aβ42 at 37 °C for 5 h. Apparently, the level of Aβ uptake by astrocytes increased in the presence of LPL at concentrations of 2 to 5 μg/ml (Fig. 2*C*, lysate). Consistent with the increase in the level of cellular uptake of Aβ, the level of Aβ remaining in culture medium was decreased (Fig. 2*C*, medium). The Aβ levels in the cell lysate quantified are shown in Fig. 2*D*, indicating that Aβ levels were significantly increased by 5–8-fold that in astrocytes incubated without LPL. Next,

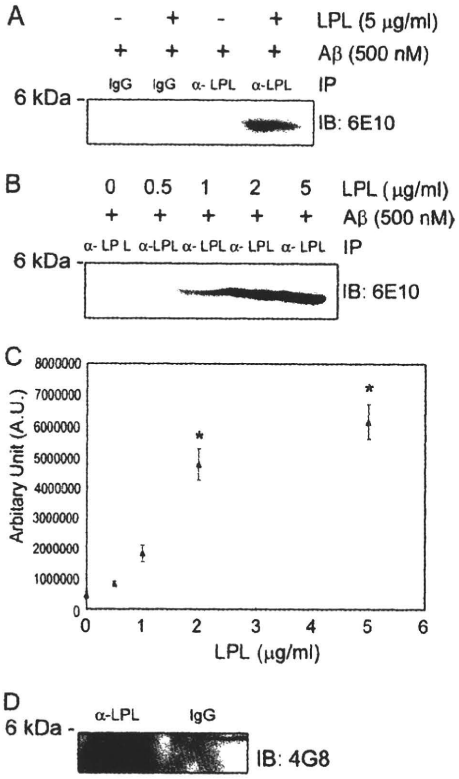

FIGURE 1. **LPL binds to Aβ *in vitro*.** *A*, LPL (5 μg/ml) and Aβ (500 nM) were incubated in DMEM at 37 °C for 3 h. Protein complexes formed were immunoprecipitated with an anti-LPL antibody (α-LPL), and the immunoprecipitates (*IP*) were analyzed by Western blotting using 6E10, an anti-Aβ antibody. These data are representative of three independent experiments. *B*, LPL at various concentrations of 0, 0.5, 1, 2, and 5 μg/ml and Aβ at 500 nM were incubated in DMEM at 37 °C for 3 h. Protein complexes formed were immunoprecipitated with an α-LPL, and the immunoprecipitates were subjected to Western blotting using 6E10. *C*, quantification of Aβ immunoprecipitated with α-LPL. The data presented are the means ± S.D. of three independent experiments. *, $p < 0.001$ *versus* samples without LPL treatment. *D*, the mouse cerebrum was homogenized by sonication in 4 volumes of PBS containing a protease inhibitor mixture and centrifuged at 1000 × *g* for 10 min at 4 °C. The supernatants were harvested. LPL-Aβ complexes in the supernatant were immunoprecipitated with an α-LPL, and the Aβ in the immunoprecipitates was detected by Western blotting using 4G8, an anti-Aβ antibody. *IB*, immunoblot.

we determined the time-dependent effect of LPL-mediated Aβ uptake into astrocytes. Astrocyte cultures were incubated with Aβ (500 nM) and LPL (2 μg/ml) at 37 °C for various hours, and the Aβ level in the cell lysate was determined. The level of Aβ in the cell lysate increased in a time-dependent manner (Fig. 2*E*). The Aβ levels in the astrocytes incubated for 3 and 5 h were significantly higher by 9–14-fold of that in astrocytes incubated without LPL (Fig. 2*F*). These concentrations of LPL are comparable with the concentrations with which LPL could act as "bridging molecules" (2, 20). There were no significant differences among the values for cultures without LPL (one-way ANOVA, $p = 0.1386$). No change in cellular morphology or cell number in astrocyte cultures was observed during the incubation (data not shown). To examine the involvement of LPL expressed by astrocytes, we carried out experiments using the gene silencing technique for LPL. The transient knockdown of LPL expression was achieved by the transfection of siRNA specific for LPL. After transfection,

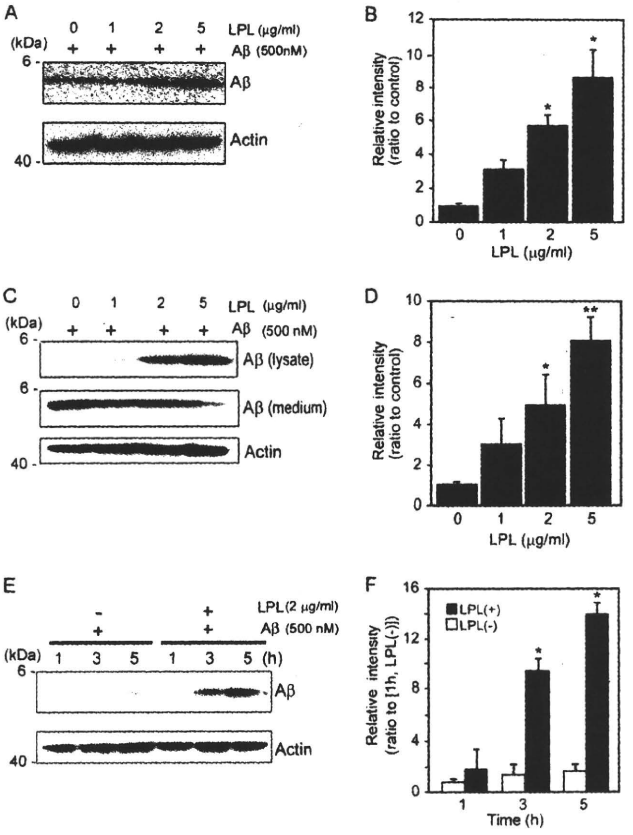

FIGURE 2. **LPL augments cell-surface association and cellular uptake of Aβ in astrocytes.** *A*, mouse primary astrocytes were incubated with LPL (0–5 μg/ml) and Aβ (500 nM) at 4 °C for 3 h. The astrocytes were washed in cold PBS three times, and the cells were harvested using a scraper. The level of Aβ on the cell surface was determined by Western blotting in a detergent extract of whole cells. *B*, quantification of cell-surface-associated Aβ. The data are the means ± S.D. of three independent experiments. *, $p < 0.001$ *versus* LPL at 0 μg/ml. *C* and *D*, astrocytes were incubated with Aβ (500 nM) and LPL (0, 1, 2, and 5 μg/ml) at 37 °C for 3 h. The cultured cells were then washed thoroughly in PBS for three times, and the cells were collected. The level of Aβ in the whole cell lysate (*lysate*), and the conditioned medium of cultured cells (*medium*) were determined by Western blotting using 6E10 antibody. The level of actin demonstrated by Western blotting using an anti-β-actin antibody was used as the loading control. These data are representative of at least three independent experiments. *D*, quantification of cellular Aβ is shown. The data presented are the means ± S.D. of three independent experiments. *, $p < 0.05$; **, $p < 0.01$ *versus* LPL at 0 μg/ml. *E* and *F*, astrocytes were incubated with Aβ (500 nM) and LPL (2 μg/ml) at 37 °C for 0, 3, and 5 h. The cultured cells were then washed thoroughly in PBS three times, and the cells were collected. The amount of Aβ in the whole cell lysate was determined by Western blotting using 6E10 antibody. The level of actin demonstrated by Western blotting using the anti-β-actin antibody was used as the loading control. These data are representative of at least three independent experiments. *F*, quantification of cellular Aβ is shown. The data are the means ± S.D. of three independent experiments. *, $p < 0.001$ *versus* LPL (+) at 1 h.

cells were treated with Aβ42 (1 μM) and then incubated at 4 °C for 3 h. As shown in Fig. 3, the cellular binding of Aβ42 to astrocytes was significantly decreased by LPL protein knockdown.

Degradation of Internalized Aβ in a Lysosomal Pathway in Astrocytes—Next, we examined the degradation of internalized Aβ. Mouse primary astrocytes were incubated with soluble Aβ42 and LPL at 37 °C for 5 h, washed in DMEM three times, and cultured at 37 °C for additional time (0, 3, 5, 12,

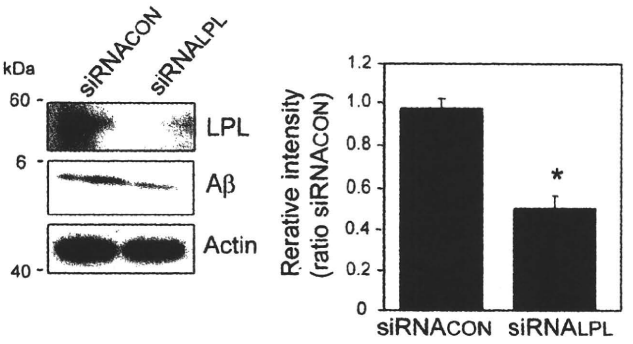

FIGURE 3. **Effect of LPL knockdown on cell-surface association of Aβ in cultured astrocytes.** Astrocytes were transfected with 10 nM siRNA specific for LPL (*siRNALPL*) and control siRNA (*siRNACON*). Forty-eight hours after transfection, cells were treated with Aβ42 (1 μM) at 4 °C for 3 h. The cells were washed in cold PBS three times, and the cells were harvested using a scraper. The level of Aβ42 on the cell surface was determined by Western blotting in a detergent extract of whole cells. The graph shows the levels of cell-surface-associated Aβ. The data are the means ± S.D. of three independent experiments. *, $p < 0.001$ *versus* control siRNA by unpaired Student's *t* test.

and 24 h). Cells were then harvested, and the Aβ level in the cell lysate was analyzed by Western blotting. The strong signal representing internalized Aβ during the initial incubation for 5 h was detected in the cell lysate at the point of 0 min after washing (Fig. 4*A*). Three to five hours after washing, the level of Aβ remaining in the cell lysate partially disappeared (Fig. 4*A*). Twelve and twenty-four hours after washing, the internalized Aβ completely disappeared, indicating that the internalized Aβ was degraded in astrocytes in a time-dependent manner (Fig. 4*A*). To gain insight into the degradation pathway of the internalized Aβ, we investigated the localization of Aβ by immunocytochemical analysis. Mouse primary astrocytes were plated on poly-L-lysine-coated coverglasses and incubated with Aβ42 (500 nM) and LPL (2 μg/ml) at 37 °C for 5 h. In some experiments, cells were washed in DMEM three times and further incubated in serum-free DMEM for 3 h. Cells were then permeabilized and stained with an anti-Aβ antibody, 6E10, and an anti-LAMP2 antibody, whose staining signal is considered as a marker of late endosomes/lysosomes (21). We found that some portions of anti-Aβ antibody-positive signals were co-localized with staining signals reactive to the anti-LAMP2 antibody, showing that the internalized Aβ was trafficked into late endosomal/lysosomal compartments (Fig. 4*B*). To confirm the involvement of a lysosomal pathway in the degradation of LPL-mediated internalized Aβ, we determined the effect of chloroquine on the localization of Aβ internalized in an LPL-mediated manner. Chloroquine is a weak base and is taken up by cells, which results in the neutralization of acidic organelles such as lysosomes and impairment of their functions (22, 23). Chloroquine treatment at concentrations of 25 and 50 μg/ml prevented the degradation of internalized Aβ 12 h after washing out (Fig. 4*C*). We also tested inhibitors of neprilysin, an insulin-degrading enzyme, and cathepsin B, all of which are known to degrade Aβ. These inhibitors failed to suppress the degradation of internalized Aβ in astrocytes (data not shown). Thus, Aβ internalized in an LPL-mediated manner was degraded in a lysosomal pathway in astrocytes.

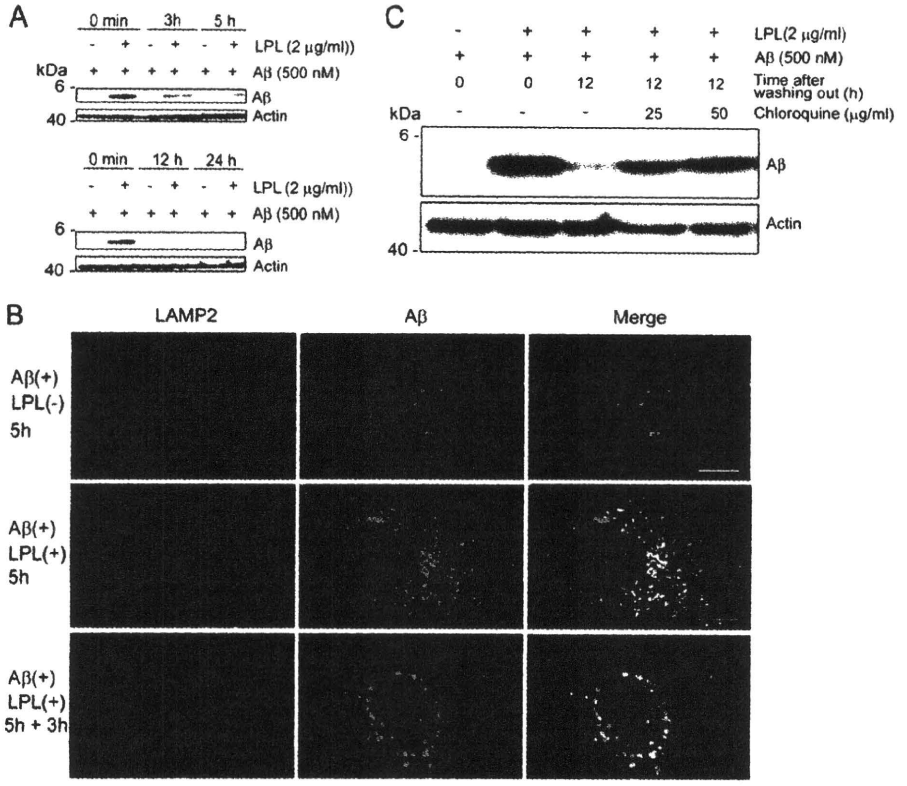

FIGURE 4. **Aβ is trafficked to late endosomal/lysosomal compartments and degraded after the LPL-mediated uptake.** *A*, mouse primary astrocytes were incubated with LPL (2 μg/ml) and Aβ (500 nM) at 37 °C for 5 h. Cells were washed in DMEM three times and then incubated in DMEM at 37 °C for 0, 3, 5, 12, and 24 h. The amount of Aβ remaining in the cells was determined by Western blotting using the anti-Aβ antibody, 6E10, in a detergent extract of whole cells. *B*, astrocytes were plated on poly-L-lysine-coated coverglasses and incubated with LPL (2 μg/ml) and Aβ (250 nM) at 37 °C for 5 h. Then, cells were permeabilized and double stained with an anti-LAMP2 antibody and 2C8. Bound antibodies were visualized with Cy3-conjugated (*red*) and FITC-conjugated (*green*) secondary antibodies for the anti-LAMP2 antibody and 6E10, respectively. Astrocytes incubated without Aβ did not show any anti-Aβ antibody-positive signals (not shown). *Scale bar*, 10 μm. *C*, astrocytes were incubated with LPL (2 μg/ml) and Aβ (500 nM) at 37 °C for 5 h. Cells were then washed in DMEM and cultured with or without chloroquine in DMEM at 37 °C for an additional 12 h. The level of Aβ in the detergent extract of whole cells was determined by Western blotting with 6E10. These are representative data of at least three independent experiments.

LPL Promotes Cellular Uptake of Aβ in a Heparan Sulfate- and Chondroitin Sulfate-dependent Manner—LPL has a high affinity with heparan sulfate (HS) and chondroitin sulfate (CS) (5, 24, 25). Therefore, we next investigated whether HS and CS are involved in the LPL-mediated cellular binding and cellular uptake of Aβ in astrocytes. Mouse primary astrocytes were pretreated with a mixture of heparinase II and heparinase III and/or chondroitinase ABC for 24 h at 37 °C, followed by incubation with Aβ42 and LPL at 4 °C for 3 h. There were no significant differences among the values in the absence of LPL (one-way ANOVA; $p = 0.0929$ for cell-surface-associated Aβ, $p = 0.4350$ for cellular Aβ). Pretreatment with heparinases or chondroitinase ABC partially decreased the level of LPL-mediated cellular binding of Aβ in astrocytes to 40 or 50% of that observed in the nontreated control, respectively (Fig. 5*A*). Interestingly, pretreatment with both heparinases and chondroitinase ABC decreased the level of LPL-mediated binding of Aβ to astrocytes to 20% of that observed in nontreated control (Fig. 5*A*). Next, we determined the effect of HS and/or CS on the LPL-mediated cellular uptake of Aβ. In conjunction with the effect of LPL on Aβ binding, heparinases and chondroitinase ABC decreased the level of LPL-mediated cellular uptake of Aβ in astrocytes to 30 and 50% of that observed in the nontreated control incubated with LPL, respectively (Fig. 5*B*). Pretreatment with both heparinases and chondroitinase ABC did not show an additive effect on the attenuation of LPL-promoted Aβ uptake (Fig. 5*B*). These findings indicate that HS and CS expressed in astrocytes are involved in the LPL-mediated association of Aβ with astrocytes and Aβ cellular uptake.

To further confirm the involvement of HS and CS in LPL-mediated Aβ uptake, we incubated astrocytes with various glycosaminoglycans. Heparin, which is a structural analog of HS, substantially suppressed the effect of LPL on Aβ uptake at a concentration of 3 μg/ml (Fig. 5*C*). The suppressive effect of heparin on LPL-mediated Aβ uptake was also observed in the presence of de-*N*-sulfated heparin, whereas either de-2-*O*-sulfated heparin or de-6-*O*-sulfated heparin had no effect on LPL-mediated Aβ uptake (Fig. 5*C*). None of these heparins interfered with the interaction between LPL and Aβ (Fig. 5*D*). In addition, 4-*O*-, 6-*O*-disulfated chondroitin sulfate (3 μg/ml) completely suppressed the promotive effect of LPL on Aβ uptake (Fig. 5*E*). 4-*O*-Sulfated chondroitin sulfate and 6-*O*-sulfated chondroitin sulfate moderately attenuated the function of LPL, whereas chondroitin (a nonsulfated form of chondroitin sulfate) and 2-*O*-, 6-*O*-disulfated chondroitin

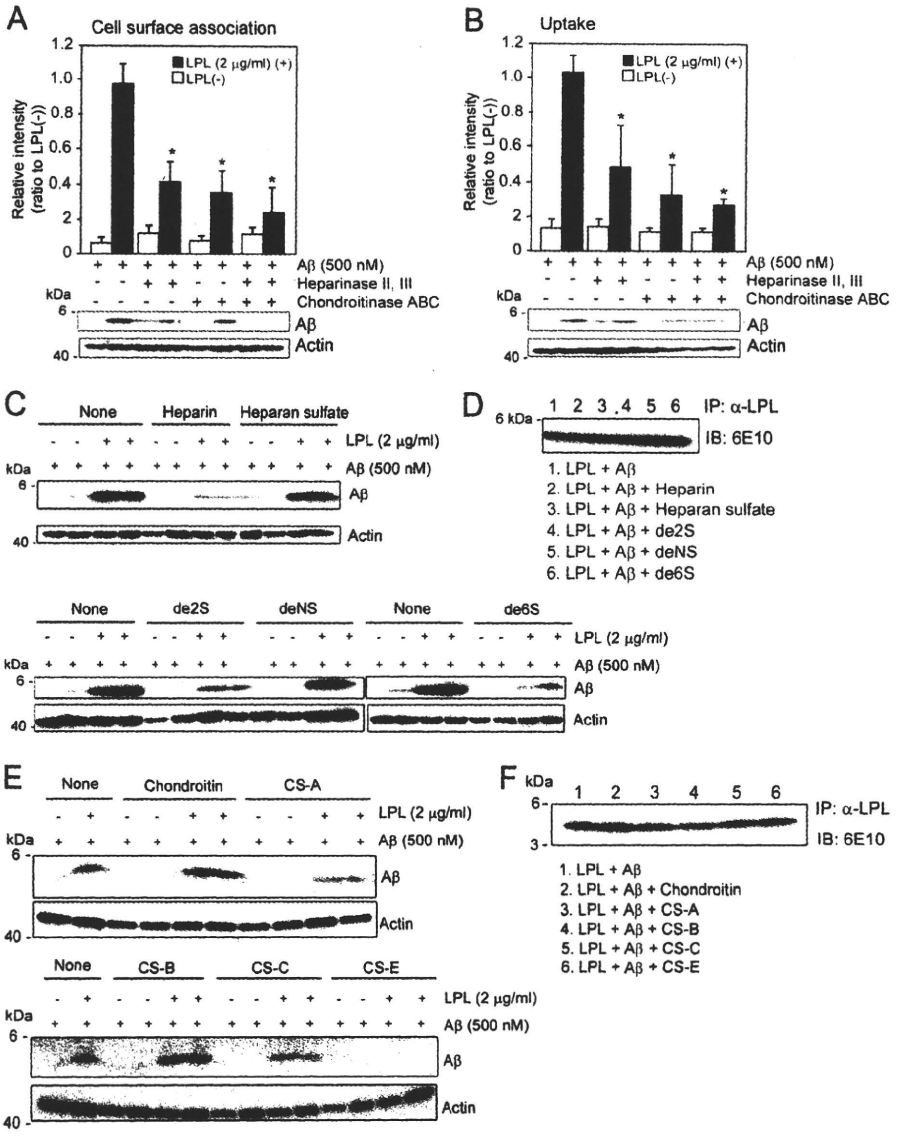

FIGURE 5. **LPL-mediated cellular binding and uptake of Aβ depends on heparan sulfate and chondroitin sulfate in astrocytes.** *A* and *B*, astrocytes from wild-type mice were pretreated with a mixture of heparinase II (0.03 μg/ml) and heparinase III (0.03 μg/ml), and/or chondroitinase ABC (0.03 μg/ml) at 37 °C for 24 h. After washing in DMEM three times, cells were incubated with LPL (2 μg/ml) and Aβ (500 nM) at 4 °C for 3 h (for cell surface association) (*A*) or 37 °C for 3 h (for uptake) (*B*). The level of Aβ in the detergent extract of whole cells was determined by Western blotting using 6E10. The quantitative assessment of cell-surface-associated Aβ (*A*) and cellular Aβ (*B*) in the present (closed bars) or absence (open bars) of LPL are shown. The data presented are the means ± S.D. of three independent experiments. * $p < 0.001$ *versus* levels of LPL (-). (*C*) Mouse primary astrocytes were incubated with Aβ (500 nM) or LPL (2 μg/ml) and Aβ (500 nM) in the presence or absence of heparin or chemically modified heparins at a concentration of 3 μg/ml at 37 °C for 5 h. The level of Aβ in the detergent extract of whole cells was determined using 6E10. (*D*) LPL (2 μg/ml) and Aβ (500 nM) were incubated in DMEM at 37 °C for 3 h in the presence or absence of heparin, heparan sulfate, or chemically modified heparins at a concentration of 3 μg/ml. Protein complexes in DMEM were immunoprecipitated (*IP*) with an anti-LPL antibody (α-LPL) and the Aβ recovered in the immunoprecipitates was analyzed by Western blotting using 6E10. These data are representative of at least three independent experiments. *de2S*, 2-*O*-desulfated heparin; *de6S*, 6-*O*-desulfated heparin; *deNS*, *N*-desulfated heparin. *E*, astrocytes were incubated with LPL (2 μg/ml) and Aβ (500 nM) in the presence or absence of chondroitin sulfates (chondroitin, chondroitin 4-sulfate (*CS-A*), 2-*O*-, 6-*O*-disulfated chondroitin sulfate (*CS-B*), 6-*O*-sulfated chondroitin sulfate (*CS-C*), and chondroitin 4,6-disulfate (*CS-E*)) at a concentration of 3 μg/ml at 37 °C for 5 h. The level of Aβ in a detergent extract of whole cells was determined by Western blotting using 6E10. *F*, LPL (2 μg/ml) and Aβ (500 nM) were incubated in DMEM at 37 °C for 3 h in the presence or absence of chondroitin sulfates at a concentration of 3 μg/ml. Protein complexes were immunoprecipitated with the anti-LPL antibody (α-LPL), and the Aβ recovered in the immunoprecipitates was analyzed by Western blotting using 6E10. The data are representative of at least three independent experiments. *IB*, immunoblot.

sulfate (also known as dermatan sulfate) did not (Fig. 5*E*). None of these CS interfered with the interaction between LPL and Aβ *in vitro* (Fig. 5*F*).

ApoE Is Dispensable for LPL-mediated Cellular Uptake of Aβ in Astrocytes—Because ApoE is reported to be involved in the metabolism of Aβ, including its aggregation and clearance (26), we analyzed the effects of ApoE on the LPL-mediated cellular uptake of Aβ in astrocytes. We collected culture media of primary astrocytes prepared from ApoE-KO mice and C57BL/6 (WT) mice. The astrocyte cultures prepared from wild-type mouse cortices were incubated in conditioned media in the presence of Aβ42 and LPL. As shown in Fig. 6A, Aβ

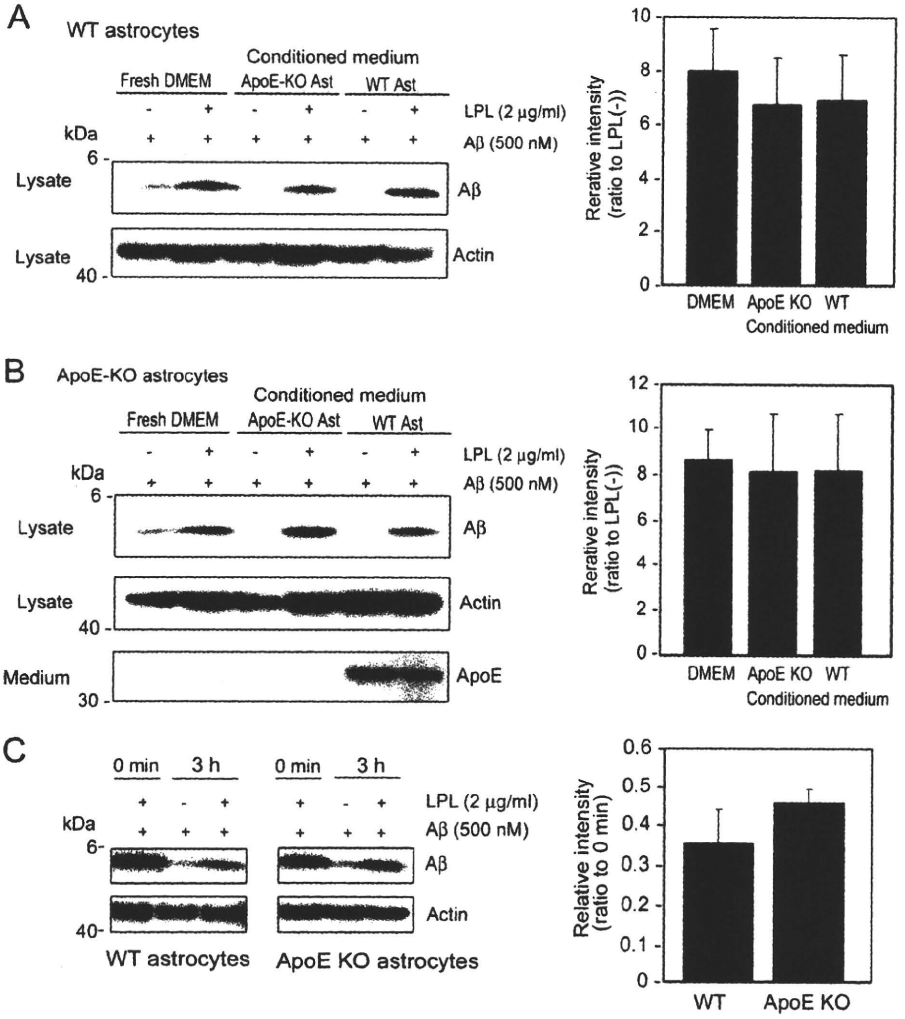

FIGURE 6. **ApoE is dispensable for the LPL-mediated cellular uptake of Aβ in astrocytes.** The astrocyte cultures prepared from WT or ApoE knock-out (KO) mice were incubated in fresh serum-free DMEM for 3 days at 37 °C. The conditioned media of these cultures were then collected. The astrocytes prepared from WT (*A*) or ApoE-KO (*B*) mouse brains were incubated in the conditioned medium of ApoE-KO astrocyte cultures or conditioned medium of WT astrocyte cultures, and LPL (2 μg/ml) and Aβ (500 nM) were added into each culture; the cultures were then maintained for another 5 h at 37 °C. After the incubation, the cultures were harvested, and the amount of cellular Aβ in a detergent extract of whole cells (*lysate*) was determined by Western blotting using 6E10. The amount of ApoE in the conditioned medium of cultured cells (*medium*) was determined by Western blotting using an anti-ApoE antibody, AB947. These data are representative of at least three independent experiments. The graphs show the cellular Aβ levels. The data are the means ± S.D. of three independent experiments. *CM*, conditioned medium; *Ast*, astrocytes. *C*, mouse primary astrocytes from WT and ApoE-KO mice were incubated with soluble Aβ42 in the presence or absence of LPL at 37 °C for 5 h, washed in DMEM three times, and further incubated at 37 °C for 3 h. Cells were then harvested, and the Aβ levels in the lysate was analyzed by Western blotting. The graph shows the cellular Aβ levels. The data are the means ± S.D. of three independent experiments.

uptake was promoted by LPL in astrocytes prepared from WT mice incubated in a fresh medium, the conditioned medium from ApoE-KO astrocytes, and the conditioned medium from WT astrocytes. There were no significant differences between these three groups (one-way ANOVA; $p = 0.6419$). This is also the case for ApoE-KO astrocytes (one-way ANOVA; $p = 0.9467$) (Fig. 6*B*). These findings indicate that ApoE is dispensable for the LPL-promoted cellular uptake of Aβ in astrocytes. We also examined the effects of ApoE on the degradation of internalized Aβ. Primary astrocytes from WT and ApoE-KO mice were incubated with soluble Aβ42 and LPL at 37 °C for 5 h, washed in DMEM three times, and further incubated at 37 °C for 3 h. Cells were then harvested, and the Aβ level in the cell lysate was analyzed by Western blotting. As shown in Fig. 6*C*, there were no significant differences between the levels of Aβ remaining in the lysate of WT astrocytes and ApoE-KO astrocytes ($p = 0.1031$).

DISCUSSION

Previous studies have shown that the mRNA expression of the LPL gene and the enzymatically active LPL are found in the brain in several mammalian species (6, 7, 27). However, considering that the main fraction of lipoproteins in the brain is HDL, which contains negligible or no triacylglycerols, and that the brain lacks an essential cofactor, apoCII, it is conceivable that LPL has a different function in the brain from that in the systemic circulation serving as an enzyme with the cofactor apoCII to catalyze the hydrolysis of triacylglycerols (28). In

the present study, we found a novel function of LPL serving as an Aβ binding molecule; that is, exogenous LPL binds to Aβ and promotes cellular binding and uptake of Aβ in astrocytes. The internalized Aβ was degraded within 12 h, mainly in a lysosomal pathway. Furthermore, we have demonstrated that HS and CS glycosaminoglycans are involved in the promotion of the LPL-mediated cellular uptake of Aβ in astrocytes.

Astrocytes are a major glial cell type in the CNS and play a crucial role in neuronal development, maintenance of synapse functions, and CNS repair after injury. Additionally, astrocytes have phagocytic and proteolytic activities (29, 30) and ingest Aβ (15, 31, 32). Our results indicate that LPL strongly enhances cellular uptake of Aβ, leading to increased degradation of Aβ in astrocytes. Previous studies have shown that SNPs in the coding region of the LPL gene are associated with AD development (33) and the severity of AD pathophysiological features (12), with the molecular mechanisms underlying this association remaining unknown. It may be possible that altered function of LPL shown in this study would result in impaired Aβ clearance and subsequent accumulation of Aβ, accelerating AD development. Because the accumulation of Aβ in the extracellular space is considered to trigger Aβ aggregation and deposition, the function of LPL to enhance Aβ binding, uptake, and degradation in astrocytes may decrease Aβ levels in the brain. However, because LPL is known to regulate the uptake and transport of vitamin E to the brain, of which deficiency results in increased Aβ accumulation and presynaptic defects accompanied by impaired learning and memory function *in vivo* (34, 35), there may be other possibilities as well, that the altered LPL function regulating vitamin E transport may enhance Aβ accumulation and impair synaptic function.

It has been suggested that lysosomal dysfunction plays a major role in Aβ accumulation, thereby causing neuronal cell death (36, 37) and that chloroquine, which disrupts lysosomal pH balance, enhances Aβ accumulation in a microglial cell line (38). Our results show that almost all of the internalized Aβ was localized in lysosomes and degraded in a time-dependent manner, and this degradation was markedly inhibited by the treatment with chloroquine, suggesting that Aβ was degraded mainly in a lysosomal pathway. These findings suggest that lysosomal pathways play a critical role in the degradation of Aβ that is internalized via a novel pathway as LPL-Aβ complexes by astrocytes.

It has been shown that LPL associates with lipoproteins and the formed LPL-bound lipoprotein complexes bind to cell-surface HS proteoglycans and CS proteoglycans (1, 5, 39), promoting the cellular uptake of lipoproteins by acting as a bridging molecule (2, 40). HS proteoglycans and CS proteoglycans are present in astrocytes (41–43). We found that pretreatment of astrocytes with a mixture of heparinases or chondroitinase ABC partially attenuated the LPL-mediated Aβ uptake, and cotreatment with heparinases and chondroitinase ABC completely suppressed the LPL-mediated cellular uptake of Aβ (Fig. 4), indicating that the LPL-mediated cellular uptake of Aβ is mediated via HS proteoglycans and CS proteoglycans. Interestingly, heparin, a highly sulfated form of HS, and 4-*O*-, 6-*O*-disulfated chondroitin sulfate, a highly sulfated CS, selectively suppressed the promotion of Aβ uptake in astrocytes. These findings suggest that LPL could act as a bridging molecule between not only cell-surface GAGs and lipoproteins but also cell-surface GAGs and Aβ and facilitate the cellular uptake of Aβ in astrocytes and that certain domains modified by multiple sulfate groups are necessary for LPL to function in astrocytes.

ApoE is one of the major apolipoproteins in the brain and plays a key role in lipid transport in the brain. ApoE affects the aggregation of Aβ *in vitro* (26). PDAPP and Tg2576 transgenic mice exhibit extensive cerebral Aβ deposition. When these transgenic mice lack the murine *apoE* gene, a significant decrease in amyloid plaque formation was observed (44, 45). Furthermore, two *in vitro* studies have demonstrated that ApoE can facilitate the cellular degradation of Aβ (16, 31). These lines of evidence suggest that ApoE affects Aβ metabolism. Thus, we examined whether ApoE could be involved in the LPL-mediated cellular uptake of Aβ. LPL promoted the cellular uptake of Aβ in wild-type and ApoE-deficient astrocytes in culture. The presence or absence of ApoE in the conditioned medium of astrocytes did not alter the levels of Aβ internalized in an LPL-mediated manner. These results suggest that ApoE is not required for the LPL-mediated cellular uptake of Aβ in astrocytes.

In this study, we demonstrated a novel LPL function; that is, LPL binds to Aβ and enhances the cellular uptake of Aβ in a sulfated glycosaminoglycan-dependent manner, and the internalized Aβ is degraded in a lysosomal pathway. Although further studies will be needed to confirm the role of LPL in the clearance of Aβ *in vivo*, our findings provide a new insight into the molecular pathogenesis of AD and a potential strategy for AD therapy.

REFERENCES

1. Williams, K. J., Fless, G. M., Petrie, K. A., Snyder, M. L., Brocia, R. W., and Swenson, T. L. (1992) *J. Biol. Chem.* **267,** 13284–13292
2. Mulder, M., Lombardi, P., Jansen, H., van Berkel, T. J., Frants, R. R., and Havekes, L. M. (1993) *J. Biol. Chem.* **268,** 9369–9375
3. Kreuger, J., Spillmann, D., Li, J. P., and Lindahl, U. (2006) *J. Cell Biol.* **174,** 323–327
4. Edwards, I. J., Goldberg, I. J., Parks, J. S., Xu, H., and Wagner, W. D. (1993) *J. Lipid Res.* **34,** 1155–1163
5. Edwards, I. J., Xu, H., Obunike, J. C., Goldberg, I. J., and Wagner, W. D. (1995) *Arterioscler. Thromb. Vasc. Biol.* **15,** 400–409
6. Goldberg, I. J., Soprano, D. R., Wyatt, M. L., Vanni, T. M., Kirchgessner, T. G., and Schotz, M. C. (1989) *J. Lipid Res.* **30,** 1569–1577
7. Yacoub, L. K., Vanni, T. M., and Goldberg, I. J. (1990) *J. Lipid Res.* **31,** 1845–1852
8. Eckel, R. H., and Robbins, R. J. (1984) *Proc. Natl. Acad. Sci. U.S.A.* **81,** 7604–7607
9. Havel, R. J., Fielding, C. J., Olivecrona, T., Shore, V. G., Fielding, P. E., and Egelrud, T. (1973) *Biochemistry* **12,** 1828–1833
10. Zannis, V. I., Cole, F. S., Jackson, C. L., Kurnit, D. M., and Karathanasis, S. K. (1985) *Biochemistry* **24,** 4450–4455
11. Rebeck, G. W., Harr, S. D., Strickland, D. K., and Hyman, B. T. (1995) *Ann. Neurol.* **37,** 211–217
12. Blain, J. F., Aumont, N., Théroux, L., Dea, D., and Poirier, J. (2006) *Eur. J. Neurosci.* **24,** 1245–1251
13. Iwatsubo, T., Odaka, A., Suzuki, N., Mizusawa, H., Nukina, N., and Ihara, Y. (1994) *Neuron* **13,** 45–53
14. Tanzi, R. E., Moir, R. D., and Wagner, S. L. (2004) *Neuron* **43,** 605–608
15. Wyss-Coray, T., Loike, J. D., Brionne, T. C., Lu, E., Anankov, R., Yan, F.,

Silverstein, S. C., and Husemann, J. (2003) *Nat. Med.* **9,** 453–457
16. Jiang, Q., Lee, C. Y., Mandrekar, S., Wilkinson, B., Cramer, P., Zelcer, N., Mann, K., Lamb, B., Willson, T. M., Collins, J. L., Richardson, J. C., Smith, J. D., Comery, T. A., Riddell, D., Holtzman, D. M., Tontonoz, P., and Landreth, G. E. (2008) *Neuron* **58,** 681–693
17. Majumdar, A., Cruz, D., Asamoah, N., Buxbaum, A., Sohar, I., Lobel, P., and Maxfield, F. R. (2007) *Mol. Biol. Cell* **18,** 1490–1496
18. Mandrekar, S., Jiang, Q., Lee, C. Y., Koenigsknecht-Talboo, J., Holtzman, D. M., and Landreth, G. E. (2009) *J. Neurosci.* **29,** 4252–4262
19. Michikawa, M., Gong, J. S., Fan, Q. W., Sawamura, N., and Yanagisawa, K. (2001) *J Neurosci.* **21,** 7226–7235
20. Fernández-Borja, M., Bellido, D., Vilella, E., Olivecrona, G., and Vilaró, S. (1996) *J. Lipid Res.* **37,** 464–481
21. Fukuda, M. (1991) *J. Biol. Chem.* **266,** 21327–21330
22. de Duve, C., de Barsy, T., Poole, B., Trouet, A., Tulkens, P., and Van Hoof, F. (1974) *Biochem. Pharmacol.* **23,** 2495–2531
23. Poole, B., and Ohkuma, S. (1981) *J. Cell Biol.* **90,** 665–669
24. Bengtsson, G., Olivecrona, T., Höök, M., Riesenfeld, J., and Lindahl, U. (1980) *Biochem. J.* **189,** 625–633
25. Pillarisetti, S., Paka, L., Sasaki, A., Vanni-Reyes, T., Yin, B., Parthasarathy, N., Wagner, W. D., and Goldberg, I. J. (1997) *J. Biol. Chem.* **272,** 15753–15759
26. Kim, J., Basak, J. M., and Holtzman, D. M. (2009) *Neuron* **63,** 287–303
27. Brecher, P., and Kuan, H. T. (1979) *J. Lipid Res.* **20,** 464–471
28. Koch, S., Donarski, N., Goetze, K., Kreckel, M., Stuerenburg, H. J., Buhmann, C., and Beisiegel, U. (2001) *J. Lipid Res.* **42,** 1143–1151
29. al-Ali, S. Y., and al-Hussain, S. M. (1996) *J. Anat.* **188,** 257–262
30. Hatten, M. E., Liem, R. K., Shelanski, M. L., and Mason, C. A. (1991) *Glia* **4,** 233–243
31. Koistinaho, M., Lin, S., Wu, X., Esterman, M., Koger, D., Hanson, J., Higgs, R., Liu, F., Malkani, S., Bales, K. R., and Paul, S. M. (2004) *Nat. Med.* **10,** 719–726
32. Matsunaga, W., Shirokawa, T., and Isobe, K. (2003) *Neurosci. Lett.* **342,** 129–131
33. Baum, L., Chen, L., Masliah, E., Chan, Y. S., Ng, H. K., and Pang, C. P. (1999) *Am. J. Med. Genet.* **88,** 136–139
34. Xian, X., Liu, T., Yu, J., Wang, Y., Miao, Y., Zhang, J., Yu, Y., Ross, C., Karasinska, J. M., Hayden, M. R., Liu, G., and Chui, D. (2009) *J. Neurosci.* **29,** 4681–4685
35. Nishida, Y., Ito, S., Ohtsuki, S., Yamamoto, N., Takahashi, T., Iwata, N., Jishage, K., Yamada, H., Sasaguri, H., Yokota, S., Piao, W., Tomimitsu, H., Saido, T. C., Yanagisawa, K., Terasaki, T., Mizusawa, H., and Yokota, T. (2009) *J. Biol. Chem.* **284,** 33400–33408
36. Bahr, B. A., and Bendiske, J. (2002) *J Neurochem.* **83,** 481–489
37. Nixon, R. A., Cataldo, A. M., and Mathews, P. M. (2000) *Neurochem. Res.* **25,** 1161–1172
38. Chu, T., Tran, T., Yang, F., Beech, W., Cole, G. M., and Frautschy, S. A. (1998) *FEBS Lett.* **436,** 439–444
39. Eisenberg, S., Sehayek, E., Olivecrona, T., and Vlodavsky, I. (1992) *J. Clin. Invest.* **90,** 2013–2021
40. Auerbach, B. J., Bisgaier, C. L., Wölle, J., and Saxena, U. (1996) *J. Biol. Chem.* **271,** 1329–1335
41. Hsueh, Y. P., and Sheng, M. (1999) *J. Neurosci.* **19,** 7415–7425
42. Laabs, T. L., Wang, H., Katagiri, Y., McCann, T., Fawcett, J. W., and Geller, H. M. (2007) *J. Neurosci.* **27,** 14494–14501
43. Tsuchida, K., Shioi, J., Yamada, S., Boghosian, G., Wu, A., Cai, H., Sugahara, K., and Robakis, N. K. (2001) *J. Biol. Chem.* **276,** 37155–37160
44. Bales, K. R., Verina, T., Dodel, R. C., Du, Y., Altstiel, L., Bender, M., Hyslop, P., Johnstone, E. M., Little, S. P., Cummins, D. J., Piccardo, P., Ghetti, B., and Paul, S. M. (1997) *Nat. Genet.* **17,** 263–264
45. Holtzman, D. M., Bales, K. R., Wu, S., Bhat, P., Parsadanian, M., Fagan, A. M., Chang, L. K., Sun, Y., and Paul, S. M. (1999) *J. Clin. Invest.* **103,** R15–R21

Molecular Neurodegeneration

BioMed Central

Research article

Open Access

Apolipoprotein E4 (1–272) fragment is associated with mitochondrial proteins and affects mitochondrial function in neuronal cells

Toshiyuki Nakamura[1], Atsushi Watanabe[2], Takahiro Fujino[3], Takashi Hosono[1] and Makoto Michikawa*[1]

Address: [1]Department of Alzheimer's Disease Research, National Institute for Longevity Sciences, National Center for Geriatrics and Gerontology, 36-3 Gengo, Morioka, Obu, Aichi 474-8522, Japan, [2]Department of Vascular Dementia, National Institute for Longevity Sciences, National Center for Geriatrics and Gerontology, 36-3 Gengo, Morioka, Obu, Aichi 474-8522, Japan and [3]Department of Bioscience, Integrated Center for Science (INCS), Ehime University, Shizukawa, Shigenobu-cyo, Onsengun, Ehime 791-0295, Japan

Email: Toshiyuki Nakamura - nakamu-t@nifty.com; Atsushi Watanabe - watsushi@nils.go.jp; Takahiro Fujino - tfujino@m.ehime-u.ac.jp; Takashi Hosono - t-hos@nils.go.jp; Makoto Michikawa* - michi@nils.go.jp

* Corresponding author

Published: 20 August 2009

Molecular Neurodegeneration 2009, 4:35 doi:10.1186/1750-1326-4-35

Received: 8 July 2009
Accepted: 20 August 2009

This article is available from: http://www.molecularneurodegeneration.com/content/4/1/35

Abstract

Background: Apolipoprotein E allele ε4 (apoE4) is a strong risk factor for developing Alzheimer's disease (AD). Secreted apoE has a critical function in redistributing lipids among central nervous system cells to maintain normal lipid homeostasis. In addition, previous reports have shown that apoE4 is cleaved by a protease in neurons to generate apoE4(1–272) fragment, which is associated with neurofibrillary tanglelike structures and mitochondria, causing mitochondrial dysfunction. However, it still remains unclear how the apoE fragment associates with mitochondria and induces mitochondrial dysfunction.

Results: To clarify the molecular mechanism, we carried out experiments to identify intracellular apoE-binding molecules and their functions in modulating mitochondria function. Here, we found that apoE4 binds to ubiquinol cytochrome c reductase core protein 2 (UQCRC2) and cytochrome C1, both of which are components of mitochondrial respiratory complex III, and cytochrome c oxidase subunit 4 isoform 1 (COX IV 1), which is a component of complex IV, in Neuro-2a cells. Interestingly, these proteins associated with apoE4(1–272) more strongly than intact apoE4(1–299). Further analysis showed that in Neuro-2a cells expressing apoE4(1–272), the enzymatic activities of mitochondrial respiratory complexes III and IV were significantly lower than those in Neuro-2a cells expressing apoE4(1–299).

Conclusion: ApoE4(1–272) fragment expressed in Neuro2a cells is associated with mitochondrial proteins, UQCRC2 and cytochrome C1, which are component of respiratory complex III, and with COX IV 1, which is a member of complex IV. Overexpression of apoE4(1–272) fragment impairs activities of complex III and IV. These results suggest that the C-terminal-truncated fragment of apoE4 binds to mitochondrial complexes and affects their activities, and thereby leading to neurodegeneration.

Background

It has been shown that the prevalence of Alzheimer's disease (AD) is associated with the polymorphisms of genes related to cholesterol metabolism, including *apolipoprotein E (apoE)* [1-3], *ATP-binding cassette transporter A1 (ABCA1)* [4], and *CYP46*, the gene encoding cholesterol 24-hydroxylase [5,6]. Human apoE, a 34-kDa protein with 299 amino acids, has three major isoforms, apoE2, apoE3, and apoE4 [7-9]. It is well known that the possession of apoE4 allele is a major risk factor for Alzheimer's disease (AD) [1-3]. The apoE4 allele, which is found in 40–65% of cases of sporadic and familial AD, increases the occurrence and lowers the age of onset of the disease [3,10]. In the central nervous system, apoE is one of the major lipid acceptors [11,12] and interacts with ABCA1 [13] to remove cholesterol from cells and generate high-density lipoprotein (HDL) particles [14] in an apoE-isoform-specific manner [15-18]. Because apoE-HDL is the major cholesterol supplier in the brain and the supply of HDL-cholesterol is essential for synaptogenesis and neurite outgrowth in neurons [19,20], the apoE-isoform-dependent difference in HDL generation may result in the apoE-isoform-dependent difference in the maintenance of synaptic plasticity and the recovery of neurons from neuronal damage found in AD brains.

In addition to the role of apoE in modulating extracellular lipid transport, the isoform-dependent intracellular functions of apoE have also been reported. A previous report has shown that apoE3 recycling is associated with concomitant cholesterol efflux and thereby contributes to the formation of apoE-containing HDL, whereas apoE4 recycling is impaired and apoE4 accumulates within endosomal compartments, inducing an impaired cholesterol efflux [21], which may lead to the accumulation of cellular cholesterol and enhanced amyloid β-protein (Aβ) generation [22]. Another effect of reduced recycling of apoE4 is due to the tight binding of apoE4 to LDLR and LRP1 in the endosomal compartment [21], which in turn affects the interaction of the amyloid precursor protein (APP) and LRP1 that is crucial for the generation of Aβ [23,24]. Other lines of evidence have shown that apoE is cleaved by a protease to generate C-terminal-truncated fragments of apoE (residues 1–272) (apoE4(1–272)) in cultured neuronal cells, and the apoE(1–272) fragment is found in the brains of AD patients and transgenic mice expressing human apoE [25,26]. This proteolytic cleavage occurs in neurons, but not in astrocytes, and C-terminal-truncated fragments of apoE accumulated in an age-dependent manner in the brains of apoE4 mice and, to a significantly lesser extent, apoE3 mice [26]. These fragments, particularly apoE4(1–272), cause AD-like neurodegeneration and memory deficits in transgenic mice expressing apoE4(1–272) [27]. These lines of evidence suggest that the intraneuronal proteolytic processing of apoE could enhance the neuropathology and promote neurodegeneration in AD brains. It has been shown that the presence of a lipid-binding region of apoE (residues 244–272) is critical for apoE fragments to exert neurotoxicity in vivo [27]. Previous studies have shown that residues 267–299 are responsible for the tetramerization of apoE in solution, and the truncation of residues 273–299 in apoE4 gives rise to the monomeric form [28], and that these hydrophobic residues appear to be responsible for the neurotoxicity caused by the C-terminal-truncated apoE4 fragments [29]. In addition to the strong neurotoxicity caused by the apoE4(1–272) fragment, it has been shown that the apoE4(1–272) fragment accumulates in filamentous neurofibrillary tanglelike structures with phosphorylated tau in the cytosol or mitochondria, inducing mitochondrial dysfunction [25-27,29]. However, it still remains unclear how the apoE fragments are transported to the filamentous cytoplasmic structures or to mitochondria, and how they associate with mitochondria and induce mitochondrial dysfunction. To address these questions, we performed experiments to identify the proteins that associate with apoE4(1–272) or intact apoE4(1–299), and determine their functions. We identified three apoE4-binding proteins, all of which are components of mitochondria. We found that these proteins preferentially bind to apoE4(1–272) than to apoE4(1–299) and that the overexpression of apoE4(1–272) fragment decreases the enzymatic activities of mitochondrial respiratory complexes III and IV in cultured cells.

Results

Identification of apoE4-associated proteins

To identify molecules that specifically bind to apoE4, various fractions obtained from mouse brain were loaded onto a FLAG-apoE4(1–272) or FLAG-apoE4(1–299) affinity column. The proteins bound to these columns were eluted with an excess amount of FLAG peptide and the extracts were subjected to SDS-PAGE and silver staining. When each mouse brain fraction was loaded onto a FLAG-apoE4(1–272) or FLAG-apoE4(1–299) affinity column and eluted samples were subjected to SDS-PAGE, many protein bands were detected as candidate apoE4-associated proteins (Fig. 1). These bands were detected only when the mouse brain fractions and FLAG-apoE4 recombinant proteins coexisted.

To identify these proteins, the protein bands were subjected to LC-MS/MS analysis. As a result, we identified sixteen apoE4-associated proteins, which are shown in Table 1. These candidate proteins include the ATP synthase protein α and β subunits, which were previously reported [30]. Interestingly, ten among the candidate proteins are shown to be associated with mitochondria.

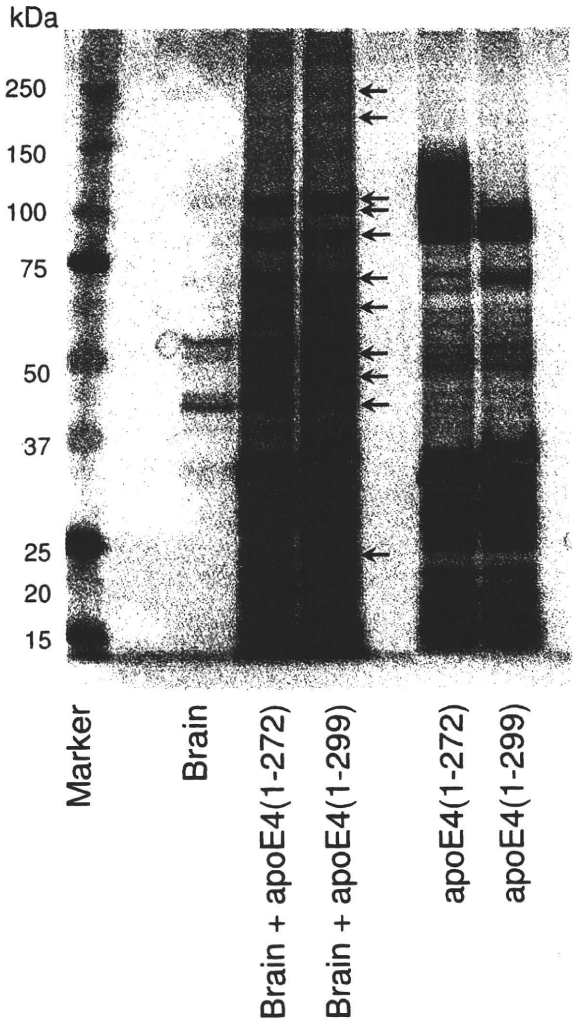

Figure 1
The proteins coimmunoprecipitated with apoE4 in the membrane extracts from mouse brain. Mouse brain membrane extracts were applied to the FLAG-apoE4(1–299) or FLAG-apoE4(1–272)-anti-FLAG M2-agarose affinity resin column and then eluted with the elution buffer. The eluant was dialyzed against the dialysis buffer, concentrated, and subjected to SDS-PAGE. The gels were stained with SilverQuest Silver Staining kit (Invitrogen). The protein bands (arrows), which were absent in the brain samples without apoE4s, and in the apoE4s samples without brain, were subjected to LC-MS/MS analysis.

Association of identified proteins with apoE4 in cultured cells

Next, we examined whether these proteins really associate with apoE in living cells. We cotransfected each candidate protein and FLAG-apoE4 into Neuro2a cells. Twenty-four hours following the transfection, the cells were harvested and treated with Triton X-100 solubilization buffer to obtain cell lysate as described in Materials and Methods. We carried out immunoprecipitation using these samples with an anti-FLAG antibody. The immunoprecipitate was then subjected to western blotting analysis using antibody specific for each protein or anti-HA antibody. This is because, in case we could not find antibodies specific for some candidate proteins, we could still generate HA-tagged proteins. Among the proteins identified by LC-MS/MS analysis, we found that three proteins, ubiquinol cytochrome c reductase core protein 2 (UQCRC2), cytochrome C1, and cytochrome *c* oxidase subunit 4 isoform 1 (COX IV 1) were associated with apoE4(1–299) and apoE4(1–272).

To examine whether mouse UQCRC2 is really associated with apoE proteins in cells, Neuro2a cells were cotransfected with mammalian expression plasmids encoding FLAG-apoE4(1–272) or FLAG-apoE4(1–299) and plasmids encoding mouse UQCRC2. Western blot analysis showed that the signal representing mouse UQCRC2 was clearly detected in the immunoprecipitate from the cells cotransfected with apoE4(1–272), while a very faint signal for UQCRC2 was detected in that from the cells cotransfected with apoE4(1–299). ApoE proteins were similarly immunoprecipitated in both samples (Fig. 2A). These results suggest that UQCRC2 prefers to associate with apoE4(1–272) than with apoE4(1–299).

To examine whether human UQCRC2 also associates with apoE4, we performed an experiment using human HA-tagged UQCRC2 expression vector. Similar to the results using mouse UQCRC2-transfected cells, the signals representing human HA-tagged UQCRC2 were clearly detected in the immunoprecipitate from the cells cotransfected with apoE4(1–272), while a very faint signal for HA-UQCRC2 was detected in that from the cells cotransfected with apoE4(1–299). Under these conditions, apoE4(1–272) and apoE4(1–299) proteins were similarly immunoprecipitated in both samples (Fig. 2B).

Next, we examined the association of human cytochrome C1 and apoE proteins using Neuro2a cells cotransfected with HA-tagged human cytochrome C1 expression vector and plasmids encoding FLAG-apoE4(1–272) or FLAG-apoE4(1–299). A strong signal for HA-tagged human cytochrome C1 was detected in the immunoprecipitate from the cell samples expressing apoE4(1–272), while a very faint signal for cytochrome C1 was detected in those transfected with apoE4(1–299) plasmid. ApoE4(1–272) and apoE4(1–299) proteins were similarly detected in both samples (Fig. 2C).

In addition, whether COX IV 1 is associated with apoE was determined. Human COX IV 1 was immunoprecipitated in the samples from apoE4(1–272)-expressing cells

Table 1: ApoE-associated proteins identified by LC-MS/MS analysis

Protein	Intracellular localization	Function
Solute carrier family 25 (mitochondrial carrier, Aralar) member 12	Mitochondria	Calcium-dependent mitochondrial aspartate and glutamate carrier
Ubiquinol cytochrome c reductase core protein I	Mitochondria	Mitochondrial electron transport
* Ubiquinol cytochrome c reductase core protein 2 (UQCRC2)	Mitochondria	Mitochondrial electron transport
* Cytochrome C1	Mitochondria	Mitochondrial electron transport
Cytochrome oxidase subunit II	Mitochondria	Mitochondrial electron transport
* Cytochrome c oxidase subunit IV isoform 1 (COX IV1)	Mitochondria	Mitochondrial electron transport
ATP synthase, H+ transporting, mitochondrial F1 complex, α subunit, isoform 1	Mitochondria	ATP synthesis
ATP synthase, H+ transporting, mitochondrial F1 complex, β subunit	Mitochondria	ATP synthesis
ATP synthase, H+ transporting, mitochondrial F1 complex, δ subunit	Mitochondria	ATP synthesis
Methylenetetrahydrofolate dehydrogenase (NADP+ dependent)- 1 like	Mitochondria	Folic acid and derivative biosynthetic process
Syntaxin binding protein 1	Cytoplasm	Modulates exocytosis of dense-core granules
Nonmuscle myosin heavy chain	Cytoplasm	Actin filament-based movement
Tubulin, alpha 1A	Cytoplasm	Constituent of microtubules
RAB3A, member RAS oncogene family	Cytoplasm	Involved in exocytosis by regulating a late step in synaptic vesicle fusion.
Progesterone receptor membrane component 1	Plasma membrane	Receptor for progesterone
Cardiotrophin-like cytokine factor 1	Extracellular space	Cell surface receptor linked signal transduction

ApoE4-associated protein bands that were detected with SDS-PAGE were prepared and analyzed as described in the Methods. Asterisks (*) show the apoE-binding proteins identified and characterized in this study.

and a very faint signal for COX IV 1 was detected in the samples from apoE4(1–299)-expressing cells, whereas apoE4(1–272) and apoE4(1–299) proteins were similarly immunoprecipitated in both samples (Fig. 3). Interestingly, these proteins, UQCRC2, cytochrome C1, and COX IV 1, are associated more strongly with apoE4(1–272) than with apoE4(1–299). Concerning other proteins, we carried out similar experiments; however, no association of these proteins with apoE4(1–272) and apoE4(1–299) was found in cultured cells (data not shown).

The levels of apoE4 in mitochondrion-rich fraction isolated from ApoE4(1–272)- or ApoE4(1–299)-expressing cells

The results indicate that apoE4(1–272) binds to mitochondrial proteins; therefore, we next determined whether the levels of apoE4(1–272) and apoE4(1–299) are also associated with the mitochondria. We, thus, determined the levels of apoE4(1–272) and apoE4(1–299) in mitochondrion-rich fractions isolated from Neuro2a cells transfected with apoE4(1–272) or apoE4(1–299). The level of apoE4(1–272) in the pellet, a mitochondrion-rich fraction, was greater than that of apoE4(1–299) (Fig. 4). VDAC, a mitochondrion marker, was recovered in the pellet fraction (Fig. 4).

Effect of apoE4(1–272) overexpression on activities of mitochondrial respiratory complexes

It is known that UQCRC2 and cytochrome C1 are subunits of mitochondrial respiratory complex III and COX IV 1 is a subunit of mitochondrial respiratory complex IV. It

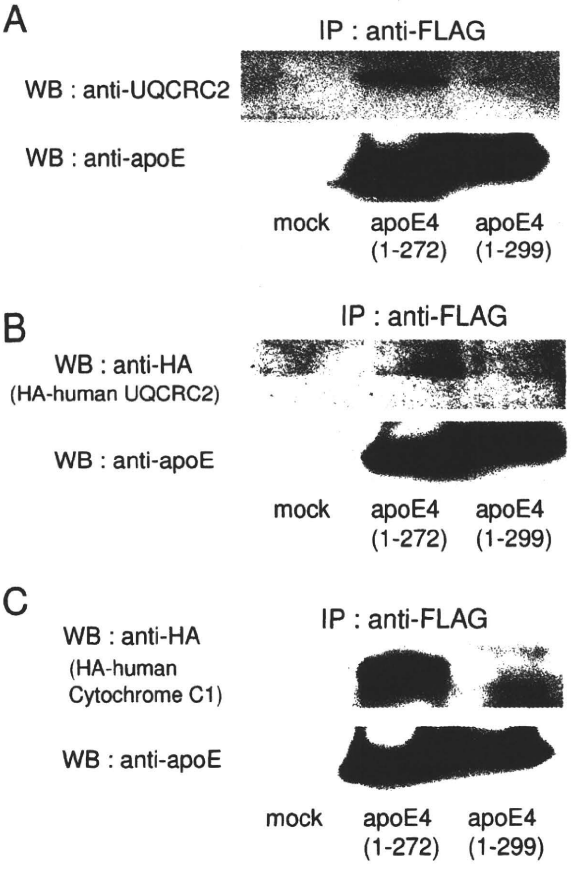

Figure 2
ApoE4 interacts with the subunits of mitochondrial respiratory complex III in Neuro2a cells. Neuro2a cells were cotransfected with mammalian expression plasmids encoding FLAG-apoE4(1–272) or FLAG-apoE4(1–299) and plasmids encoding mouse UQCRC2, human HA-UQCRC2, or human HA-cytochrome C1, all of which are candidate proteins suggested to be associated with apoE4 (Table 1). Twenty-four hours following the transfection, the cells were harvested and treated with 500 μl of Triton X-100 solubilization buffer to obtain cell lysate. The cell lysate was then incubated with anti-FLAG M2-agarose affinity resin, and the protein binding to the affinity column was eluted using FLAG peptide, and the eluted protein was then analyzed by western blotting with anti-UQCRC2 (mouse UQCRC2) antibody (A), anti-HA antibody (human UQCRC2) (B), or anti-HA antibody (human cytochrome C1) (C).

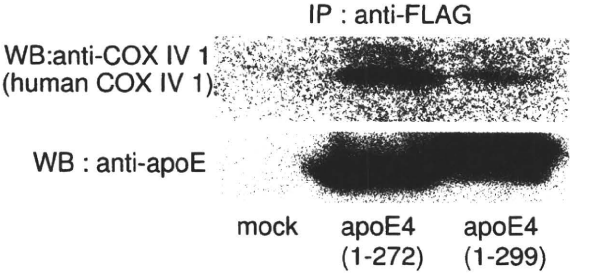

Figure 3
ApoE4 interacts with the subunits of mitochondrial respiratory complex IV in Neuro2a cells. Neuro2a cells were co-transfected with FLAG-apoE4 (1–272 or 1–299) plasmids and mammalian expression plasmids encoding the candidate apoE4-associated proteins. The cells were treated with 500 μl of Triton X-100 solubilization buffer and the cell lysate was incubated with anti-FLAG M2-agarose affinity resin. The immunoprecipitates were then analyzed by western blotting with an anti-COX IV 1 antibody (human COX IV 1).

was reported that apoE4(1–272) induces mitochondrial dysfunction [25-27,29]. Because these proteins are associated more strongly with apoE4(1–272) than with apoE4(1–299), we investigated whether the enzymatic activities of mitochondrial respiratory complexes III and IV change, when apoE4(1–272) is overexpressed in cultured cells. Complex III activity was expressed as the difference in the reduction of cytochrome *c* with or without antimycin A and myxothiazol, both of which are complex III inhibitors. Expectedly, the complex III activity of apoE4(1–272)-overexpressing Neuro2a cells was lower than that of apoE4(1–299)-overexpressing cells (Fig. 5A). Because apoE4(1–272) associates with UQCRC2 and cytochrome C1, there was a possibility that the decrease in complex III activity in Neuro2a cells expressing apoE4(1–272) was due to the interaction between apoE4 and complex III. Complex IV activity was expressed as the difference in the oxidation of ferrocytochrome C with or without KCN and Na_3N, both of which are complex IV inhibitors. The complex IV activity of apoE4(1–272)-overexpressing cells was significantly lower than that of apoE4(1–299)-overexpressing cells (Fig. 5B). The levels of the mitochondrial proteins UQCRC2 and cytochrome C1 in apoE4(1–272)- and apoE4(1–299)-overexpressing cells were similar, as demonstrated by western blot analysis using anti-UQCRC2 and anti-cytochrome C1 antibodies (Fig. 5C).

Effects of overexpression of apoE4(1–272) and apoE4(1–299) on ATP synthase activity and mitochondrial membrane potential

Because apoE4(1–272) decreases the activities of mitochondrial complexes III and IV, we next examined whether the overexpression of apoE4(1–272) also affects ATP synthase activity and mitochondrial membrane potential. Unexpectedly, apoE4(1–272) and apoE4(1–299) showed no effect on ATP synthase activity (Fig. 6A). We further examined the effect of the overexpression of

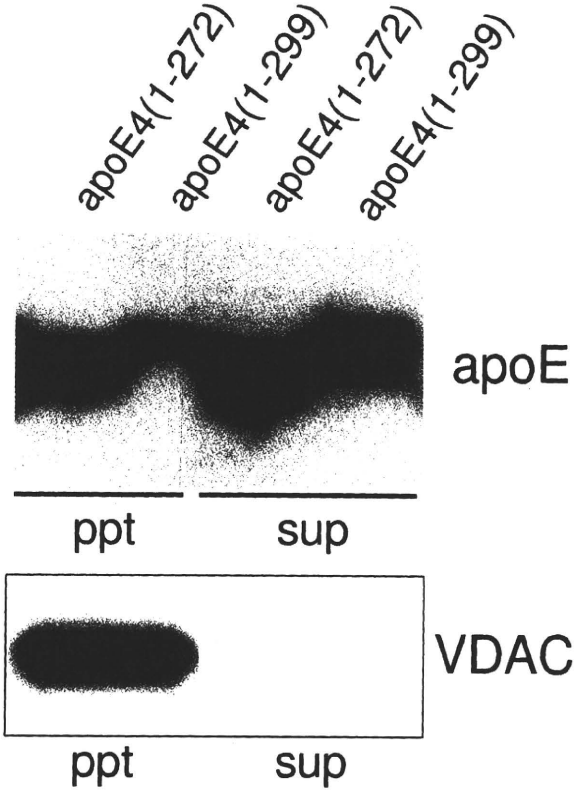

Figure 4
The level of apoE4(1–272) recovered from the mitochondrion-rich fraction is greater than that of apoE4(1–299). Neuro2a cells transfected with ApoE4(1–272) and ApoE4(1–299) plasmids were harvested and homogenized with a homogenizing buffer (10 mM Tris-HCl, pH 7.4, 1 mM EDTA, 0.25 M sucrose), and the resulting homogenate was centrifuged at 1,000 *g* for 10 min at 4°C. The resulting supernatant was further centrifuged at 8,000 *g* for 20 min at 4°C. The resulting precipitate (ppt) was used as the mitochondrion-rich fraction. Equal amounts of proteins from the ppt and supernatant (sup) fractions were analyzed by western blot analysis using the anti-apoE antibody, AB946, and the anti-VDAC antibody. VDAC was used as the mitochondrion marker.

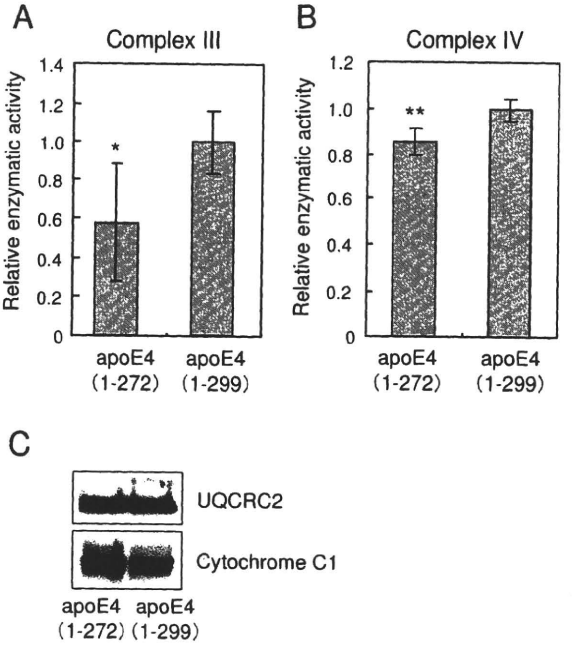

Figure 5
Overexpression of apoE4(1–272) results in the decreased level of complex III and IV activities. Enzymatic assays of respiratory chain complexes III (A) and IV (B) from Neuro2a cells overexpressing FLAG-apoE4(1–272 or 1–299) were determined as described in the Methods. The mitochondria levels in apoE4(1–272)- and apoE4(1–299)-overexpressing cells were determined by western blot analysis using the anti-UQCRC2 and the anti-cytochrome C1 antibodies (C). Data are the mean ± SEM of nine independent experiments. * $P < 0.005$, ** $P < 0.0005$ (t-distribution test).

apoE4(1–272) and apoE4(1–299) on mitochondrial membrane potential. Neuro2a cells transfected with these apoE4 species were stained with JC-1, a fluorescent dye that has been shown to be a reliable indicator of mitochondrial membrane potential changes in intact cells. After three hours of treatment of Neuro2a cells with 1 μM valinomycin, a K^+ ionophore that disrupts the transmembrane electrical gradient, the intensity of red fluorescence (FL2) markedly decreased, whereas that of green fluorescence (FL1) slightly increased, as demonstrated by JC-1 staining (Fig. 6B), indicating the dissipation of mitochondrial membrane potential. On the other hand, there were no significant differences in FL1 and FL2 intensities among Neuro2a cells transfected with mock, apoE4(1–272) and apoE4(1–299) (Figs. 6B, C, and 6D), indicating that the overexpression of apoE4(1–272) and apoE4(1–299) has no effect on mitochondrial membrane potential.

Discussion

Here, we show the molecules associated with apoE protein. Among the molecules identified, we show for the first time that apoE4, particularly C-terminal cleaved apoE4(1–272), binds to UQCRC2 cytochrome C1 and COX IV 1. Although apoE(1–272) has been shown to be translocated to mitochondria, it still remains unclear how the apoE fragments associate with mitochondria and induce mitochondrial dysfunction. The present study has shown that apoE4(1–272) binds to UQCRC2 cytochrome C1, a component of complex III, and COX IV 1, a component of complex IV, and that overexpression of apoE(1–

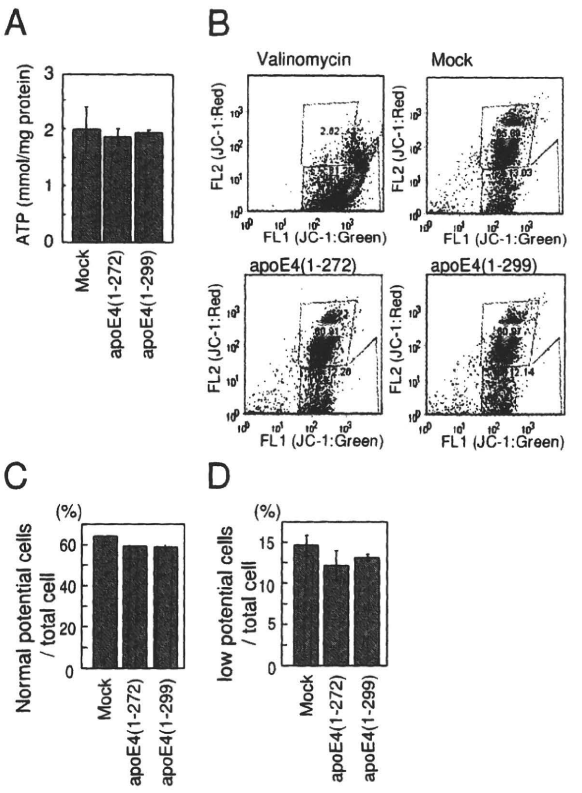

Figure 6
Effects of overexpression of apoE4(1–272) and apoE4(1–299) on ATP synthase activity and mitochondrial membrane potential. The ATP synthase activity in Neuro2a cells transfected with the ApoE4(1–272) and ApoE4(1–299) plasmids were determined (A) as described in the Methods. The data are the mean ± SEM of three experiments. (B) Flow cytometry plots were used to determine the ratio of cells having normal and low mitochondrial membrane potentials, which were demonstrated by staining with the JC-1 dye. The distribution of the cells sorted by FACS was analyzed, and the ratios of the number of cells showing normal membrane potential (C) and low membrane potential (D) to total cell number were calculated.

272) fragment in Neuro2a cells results in decreases in the levels of complex III and complex IV activities compared with those in cells overexpressing intact apoE4. These results suggest that the apoE4(1-272) fragment binds to UQCRC2 cytochrome C1 and COX IV 1, thereby inhibiting complex III and complex IV activities, respectively. The candidate molecules, which may associate with apoE to transport apoE to mitochondria, were not identified in our present analysis (Table 1). This should be addressed in a future study.

Another finding in the present study is that UQCRC2 cytochrome C1 and COX IV 1 are associated more strongly with ApoE4(1-272) than with intact apoE4(1-299) (Figs. 2, 3). There are at least two possible explanations for this result. One explanation is that apoE4(1-272) is structurally different from apoE4(1-299), resulting in the difference in hydrophobicity or binding affinity to other proteins. It has been shown that the C-terminus of apoE (residues 253–289) participates in hydrophobic interactions that stabilize the tetramer [28], and that these hydrophobic residues are suggested to be responsible for inducing neurotoxicity caused by the C-terminal-truncated apoE4 [29]. In addition, a recent study has shown that apoE4 lacking a hydrophobic C-terminal α-helical segment (residues 273–299) found in brain leads to a less organized C-terminal structure that is available for interaction with cell membranes and other proteins such as Aβ [31]. Another explanation is that more apoE(1-272) is translocated to mitochondria than intact apoE(1-299), because the silver staining shows that the intensities of the bands representing apoE-associated proteins were not different between the samples containing apoE4(1-272) and apoE4(1-299) (Fig. 1), whereas the level of apoE4(1-272) was greater than that of apoE4(1-299) in the mitochondrion-rich fraction of Neuro2a cells expressing apoE4(1-272) and apoE4(1-299) (Fig. 4). Although the precise mechanism underlying this difference is yet unknown, it is possible that the truncation of residues 273–299 in apoE4 leads to the reorganization of the C-terminal domain, with a lipid-binding region being less organized and available for hydrophobic interaction including Aβ [31-33].

Regarding the mitochondrial dysfunction in Alzheimer disease, there are previous reports showing that the overexpression of amyloid precursor protein increases the level of Aβ in mitochondria [34], and that mitochondrial complex III and IV activities are decreased in Tg2576 mouse brains [34]. In addition, the complex IV activity was shown to decrease in the brain of AD patients [35-39]. Moreover, it has been shown that the apoE(1-272) fragment is generated at a greater level from apoE4 than apoE3, and the overexpression of apoE isoform-dependently affects mitochondrial function [27]. These lines of evidence together with our present study suggest that the greater level of apoE4(1-272) fragment generated from apoE4 may be associated with Aβ that is transported to mitochondria and binds to UQCRC2 cytochrome C1 and COX IV 1, and causes mitochondrial dysfunction.

Complexes III and IV are related to ATP synthesis and the maintenance of mitochondrial membrane potential, which are critical for cell survival. Thus, we examined the